

Arenethiolate Monolayer-Protected Gold Clusters

Shaowei Chen[†] and Royce W. Murray*

Kenan Laboratories of Chemistry, University of North Carolina,
Chapel Hill, North Carolina 27599-3290

Received July 6, 1998. In Final Form: October 29, 1998

Nanometer-sized gold clusters stabilized by monolayers of arenethiolates prepared using the Brust reaction are somewhat larger (by TEM) and less thermally stable (by TGA) than those prepared under similar conditions and stabilized by alkanethiolates. Like the latter, the mean core size decreases for synthetic conditions based on larger thiol/Au ratios. The differential pulse voltammetry of the arenethiolates was especially interesting by displaying electrochemical ensemble Coulomb staircase features analogous to those recently reported, even in unfractionated cluster preparations, consistent with a smaller dispersity of core sizes than usual for alkanethiolate-protected clusters. The spacings between quantized capacitance charging features on the potential axis decrease with decreasing methylene linker chain length. TEM studies show chain/ring self-organization features. The UV-vis spectral surface plasmon bands of the arenethiolate clusters are virtually independent of the specific aryl ligands for small cluster sizes; for others a collective band feature might be due to the formation of small aggregates of MPCs.

Interest in nanometer-sized metal clusters protected from aggregation in solvent-free forms has been intense^{1–3} since the report by Brust et al.⁴ of the nonaqueous synthesis of a stable, dodecanethiolate monolayer-protected cluster (MPC) of gold atoms. The Brust reaction can be used to prepare alkanethiolate-MPCs over a range of monolayer chain-lengths and with Au core sizes that are much smaller than those for well-known aqueous Au colloids.² The current interest in alkanethiolate-MPCs has been divided into efforts directed at properties of the metal core,⁵ of the monolayer surrounding the core,⁶ of ω -functional groups that can be placed onto the alkanethiolate monolayers,^{7,8} and of the reactivity of these ω -functionalities.^{7,8} The high level of interest in MPCs is vested (a) in the lack of prior examples of unequivocally stable and isolable metal clusters in the nanometer size range, (b) in the potentialities of MPCs in the diverse areas of electrocatalysts,⁹ optoelectronic devices, chemical sensors and biosensors,^{1–3} (c) as a new avenue to study of size-dependent properties such as metal vs. molecular behavior,¹⁰ and (d) in the general absence of (and need for) a broader, rational, synthetic chemistry for systematically making and modifying nanoparticles.

The focus on MPCs stabilized by alkanethiolate monolayers has been facilitated by the extensive existing literature of self-assembled monolayers that alkanethiols readily form on flat Au surfaces.^{11,12} In contrast, the literature on forming monolayers with arenethiols on flat Au surfaces and on MPCs is quite limited. Work by Tao et al.¹³ shows that arenethiols do not readily form highly ordered assemblies, while Brust et al.^{14a} showed that *p*-mercaptophenol could be used to prepare 5 nm diameter

(mean) MPCs in methanol. Ulman et al.^{14b} reported stabilization of Au nanoparticles with C₂₂H₄₅-SO₂-C₆H₄-O-C₄H₈-SH, but the influence of the aromatic moiety in this case was moderated by the large methylene group monolayer content.

This paper describes the Brust reaction⁴ synthesis and characterization of a series of arenethiolate-MPCs based on phenethyl mercaptan, benzylthiol, thiophenol, 4-thiocresol, and 2-naphthalenethiol. The resulting arenethiolate-MPCs are stable in solvent-free forms (although less so than alkanethiolate-MPCs). The Au core sizes resulting from the arenethiolate-MPC preparation are less polydisperse than the usual alkanethiolate-MPC preparations;⁵ this allows observations of quantized capacitance charging (Coulomb staircase) behavior even

(5) (a) Leff, D. V.; Ohara, P. C.; Heath, J. R.; Gelbart, W. M. *J. Phys. Chem.* **1995**, *99*, 7036. (b) Kreibitz, U.; Vollmer, M., Ed., *Optical Properties of Metal Clusters*; Springer-Verlag: New York, 1995. (c) Vezmar, I.; Alvarez, M. M.; Khoury, J. T.; Salisbury, B. E.; Whetten, R. L. *Z. Phys. D* **1997**, *40*, 147. (d) Hostetler, M. J.; Wingate, J. E.; Zhong, C.-J.; Harris, J. E.; Vachet, R. W.; Clark, M. R.; Londono, J. D.; Green, S. J.; Stokes, J. J.; Wignall, G. D.; Glish, G. L.; Porter, M. D.; Evans, N. D.; Murray, R. W. *Langmuir* **1998**, *14*, 17.

(6) Hostetler, M. J.; Stokes, J. J.; Murray, R. W. *Langmuir* **1996**, *12*, 2, 3604.

(7) (a) Hostetler, M. J.; Green, S. J.; Stokes, J. J.; Murray, R. W. *J. Am. Chem. Soc.* **1996**, *118*, 4212. (b) Green, S. J.; Stokes, J. J.; Hostetler, M. J.; Pietron, J. J.; Murray, R. W. *J. Phys. Chem. B* **1997**, *101*, 2663.

(8) Ingram, R. S.; Hostetler, M. J.; Murray, R. W. *J. Am. Chem. Soc.* **1997**, *119*, 9175.

(9) (a) Ingram, R. S.; Murray, R. W. *Langmuir* **1998**, *14*, 4115–4121. (b) Pietron, J. J.; Murray, R. W. Unpublished results, UNC, 1998.

(10) (a) Chen, S.; Ingram, R. S.; Hostetler, M. J.; Pietron, J. J.; Murray, R. W.; Schaaff, T. G.; Khoury, J. T.; Alvarez, M. M.; Whetten, R. L. *Science* **1998**, *280*, 2098. (b) Chen, S.; Murray, R. W.; Feldberg, S. W. *J. Phys. Chem. B*, in press.

(11) For reviews, see: (a) Ulman, A. *An Introduction to Ultrathin Organic Thin Films from Langmuir-Blodgett to Self-Assembly*; Academic Press: New York, 1991. (b) Whitesides, G. M.; Laibinis, P. E. *Langmuir* **1990**, *6*, 87.

(12) (a) Nuzzo, R. G.; Allara, D. L. *J. Am. Chem. Soc.* **1983**, *105*, 4481. (b) Porter, M. D.; Bright, T. B.; Allara, D. L.; Chidsey, C. E. D. *J. Am. Chem. Soc.* **1987**, *109*, 3559. (c) Bain, C. D.; Whitesides, G. M. *Angew. Chem., Int. Ed. Engl.* **1989**, *28*, 506. (d) Widrig, C. A.; Chung, C.; Porter, M. D. *J. Electroanal. Chem.* **1991**, *310*, 335.

(13) (a) Chang, S.-C.; Chan, I.; Tao, Y.-T. *J. Am. Chem. Soc.* **1994**, *116*, 6792. (b) Tao, Y.-T.; Wu, C.-C.; Eu, J.-Y.; Lin, W.-L.; Wu, K.-C.; Chen, C.-H. *Langmuir* **1997**, *13*, 4018.

(14) (a) Brust, M.; Fink, J.; Bethell, D.; Schiffrin, D. J.; Kiely, C. J. *Chem. Soc., Chem. Commun.* **1995**, 1655. (b) Johnson, S. R.; Evans, S. D.; Mahon, S. W.; Ulman, A. *Langmuir* **1997**, *13*, 51–57.

* To whom correspondence should be addressed. E-mail: rwm@net.chem.unc.edu.

[†] Present address: Department of Chemistry, Southern Illinois University, Carbondale, IL 62901.

(1) Schmid, G., Ed., *Clusters and Colloids*, VCH: Weinheim, Germany, 1994.

(2) Hayat, M. A., Ed., *Colloidal Gold: Principles, Methods, and Applications*, Academic: San Diego, CA, 1991.

(3) *Proceedings of the Robert A. Welch Foundation 40th Conference in Chemical Research: Chemistry on Nanoscale*; Houston, TX, October 1996.

(4) Brust, M.; Walker, M.; Bethell, D.; Schiffrin, D. J.; Whyman, R. *J. Chem. Soc. Chem. Commun.* **1994**, 801.

with unfractionated (as-prepared) material. The quantized double-layer capacitance behavior^{10,15} of MPCs is a fundamentally new avenue into study of interfacial phenomena.

Experimental Section

Chemicals. 2-Phenylethyl thiol (PhC2SH, 99%), benzylthiol (PhCSH, 99%), thiophenol (PhSH, 99+%), 4-thiocresol (4-CresolSH, 98%), 2-naphthalenethiol (2-NapSH, 99%), and *n*-hexanethiol (C6SH, 96+) were used as received (Aldrich), as were tetra-*n*-octylammonium bromide (98%, Aldrich), sodium borohydride (99%, Aldrich), tetra-*n*-hexylammonium perchlorate (Hx₄NClO₄, Alfa Products), and absolute ethanol (Aaper). 4-Phenylbutane-1-thiol (PhC4SH) was synthesized from 4-phenyl-1-butanol using a literature procedure,¹⁶ as was hydrogen tetrachloroaurate (from 99.999% pure gold).¹⁷ Toluene and methylene chloride (analytical reagents, Mallinckrodt), acetonitrile (Burdick & Jackson), and tetrahydrofuran (THF, J. T. Baker) were dried with 4 Å molecular sieves prior to use. Water (>18 MΩ) was obtained with a Millipore Nanopure water system.

Synthesis. Arenethiolate-MPCs were synthesized according to the Brust reaction,⁴ in which (aqueous) HAuCl₄ was phase-transferred into toluene with tetra-*n*-octylammonium bromide and reacted there first with the arenethiol and then with a large excess (10:1 relative to Au) of borohydride reducing agent. The molar ratio of thiol and chloroaurate, which influences the eventual average arenethiolate-MPC core size, was varied from 3:1 to 1:4. Reaction temperature has been reported to also influence the core dimension;⁵ the initial toluene solution temperature (before adding borohydride) was either room temperature or 0 °C. Formation of the arenethiolate-MPC was evidenced by an immediate, pronounced darkening of the toluene phase. After ca. 24 h, the toluene solvent was removed with a rotary evaporator and the resulting solid washed on a frit with ethanol and hexane to remove excess thiol. The abbreviation used here to denote reaction conditions is, for instance, PhCSAu (0 °C, 3×), which specifies that benzylthiolate-MPCs were synthesized at an initial reaction temperature of 0 °C, using a 3-fold molar excess of PhCSH over gold. The notation (room temperature, 1/4×) would indicate that the reaction was carried out at room temperature with 4-fold molar deficiency of thiol to gold.

The arenethiolate-MPCs are quite stable in solvent-free form. Long chain alkanethiolate-MPCs are waxy black solids whereas arenethiolate-MPCs are powdery in consistency. They are soluble in acetone and acetonitrile (in which alkanethiolate-MPCs are poorly soluble) but insoluble in hexane (where alkanethiolate-MPCs are very soluble). The solubility properties crudely indicate that arenethiolate-MPCs are more polar.

Transmission Electron Microscopy (TEM). TEM samples were prepared by spreading one drop of a ~1 mg/mL cluster toluene solution onto standard carbon-coated (20–30 nm) Formvar films on copper grids (600 mesh), drying in air for at least 45 min. Phase contrast images of the particles were obtained with a side-entry Phillips CM12 electron microscope operating at 120 keV. Three typical regions of each sample were imaged at 340K. Size distributions of the gold cores were obtained from digitized photographic enlargements of well-separated particles using Scion Image Beta Release 2 (available at www.scioncorp.com), where values from twins or aggregates of particles were removed manually.

Thermogravimetric Analysis (TGA). TGA was performed with a Seiko SSC 5200 thermal analysis system on samples of 15 mg or more of accurately weighed, carefully dried cluster, under N₂ and in standard aluminum pans. Temperatures were controlled from 25 to 600 °C at 20 °C/min.

Spectroscopy. ¹H NMR spectra (taken in CD₂Cl₂ with a Bruker AC200 spectrometer) serve as indicators of purification

of the arenethiolate-MPC from unbound arenethiol. Resonances of MPC monolayers are characteristically broad whereas those of unbound arenethiols and other solutes are sharp. The absence of super-imposed sharp resonances signifies adequate cleanup of the MPC product from excess of arenethiol ligands. The broad MPC spectrum of the PhC4Au cluster, for example, inhibits a broad aryl resonance at $\delta \approx 7.1$ ppm and a pair of broad methylene resonances at $\delta \approx 2.5$ and ≈ 1.7 ppm.

UV-vis spectra were observed with an ATI Unicam UV/vis spectrometer (resolution 2 nm) in CH₂Cl₂ solutions with typically 1 mg/10 mL arenethiolate-MPC concentrations in a 1 cm quartz cuvette. Infrared spectra of solid MPC films drop cast onto a KBr plate were taken with a Bio-Rad Model 6000 Fourier-transform infrared spectrometer.

Kinetics of MPC Decomposition by Cyanide. As shown previously,¹⁸ the rate at which monolayer-protected Au clusters are decomposed by cyanide provides a measure of core protection from this aggressive ligand. A 3 mL sample of a THF solution of arenethiolate-MPC (final concentration ca. 7.1 mM in cluster and 1.0 mM in Au) is quickly mixed with 0.5 mL of an aqueous NaCN solution (final concentration ca. 8.7 mM). The decay in absorbance (at $\lambda = 520$ nm; similar kinetic results are obtained at 340 nm) is monitored over at least three reaction half-lives on an ATI Unicam-4 UV/vis spectrometer, as the light brown cluster solution decomposes into one containing colorless, slightly soluble cyano-Au complexes (assumed, actual identity of Au product not determined), disulfides (~90% of the recovered organic matter) and aryl cyanides. The latter products were determined by ¹H NMR. The absorbance decay data were fit to a general first-order equation, $y = y_0 + ae^{-kt}$, where y is the experimental absorbance and y_0 is a constant term accounting for a small amount of absorbance and/or light scattering by the reaction product (i.e., loss of transmittance). More details are provided in the Results and Discussion section.

Electrochemistry. Electrochemical measurements (BAS Model 100B/W) were carried out on ca. 0.1 mM arenethiolate-MPC solutions in a (2:1 v:v) toluene/acetonitrile mixed solvent containing 0.05M Hx₄NClO₄ electrolyte. The electrodes were a 0.065 cm² Pt disk working electrode, a Ag/AgCl reference electrode, and a Pt coil counter electrode. The working electrode was polished with 1/4 μm diamond paste (Buehler) between experimental runs, followed by thorough consecutive rinsings with Nanopure water, ethanol, and acetone. The cell solution was degassed for ca. 30 min. with high purity N₂ presaturated with the mixed solvent. The PhC4SAu MPC sample used for the electrochemical observations had been fractionated¹⁹ with toluene-acetone (1:1 v:v) mixed solvent to lower the dispersity of core size; the other arenethiolate-MPCs examined were unfractionated.

Results and Discussions

We begin with a description of the quantized electrochemical charging of the arenethiolate-stabilized Au nanoparticles. The characterization of these new materials continues with TEM and TGA results on the Au core size and the monolayer structure, respectively. Results from stability and electronic spectroscopy studies follow.

Electrochemistry of Arenethiolate MPCs. In voltammetry of MPC solutions, the clusters diffusively collide with the working electrode surface and (assuming facile electron transfers) the potentials of their cores become equilibrated with that of the electrode. The current flowing for this charging process is jointly governed by the diffusive flux and double layer capacitances of the MPCs. The most interesting aspect of the capacitance charging relates to the tiny size of the capacitance of a nanometer-sized particle. The capacitance can be so small (<1 aF/cluster) that transfer of a single electron between the electrode

(15) Ingram, R. S.; Hostetler, M. J.; Murray, R. W.; Schaaff, T. G.; Khoury, J. T.; Whetten, R. L.; Bigioni, T. P.; Guthrie, D. K.; First, P. N. *J. Am. Chem. Soc.* **1997**, *119*, 9279.

(16) Bain, C. D.; Troughton, E. B.; Tao, Y.-T.; Evall, J.; Whitesides, G. M.; Nuzzo, R. G. *J. Am. Chem. Soc.* **1989**, *111*, 321.

(17) (a) Brauer, G., Ed., *Handbook of Preparative Inorganic Chemistry*; Academic Press: New York, 1965; p 1054. (b) Block, B. P. *Inorg. Synth.* **1953**, *4*, 14.

(18) Templeton, A. C.; Hostetler, M. J.; Kraft, C. T.; Murray, R. W. *J. Am. Chem. Soc.* **1998**, *120*, 1906–1911.

(19) Schaaff, T. G.; Shafiqullin, M. N.; Khoury, J. T.; Veizar, I.; Whetten, R. L.; Cullen, W. G.; First, F. N.; Gutierrez-C.; Ascencio, J.; Joseyacamán, M. J. *J. Phys. Chem. B* **1997**, *101*, 7885.

and an MPC can change the potential of the latter by measurable fractions of a volt. This phenomenon has been recently detected^{10,15} in voltammetry of solutions of monodisperse alkanethiolate-MPCs and at nanoscopic working electrodes,²⁰ and is an electrochemical analogue of the classical Coulomb Staircase experiment.²¹ The latter is carried out on a single nanoparticle whereas the electrochemical experiment involves a huge number of MPCs (those making up the diffusion layer around the electrode), hence it was termed an electrochemical ensemble Coulomb staircase. The shorter and equally apt phrase "quantized capacitance charging" is used in the present writing.

The previous quantized capacitance charging experiments^{10,15} were conducted on samples of alkanethiolate-MPCs that had been carefully fractionated¹⁹ so that their core sizes were all the same or at least resided within a narrow range of values. Under those conditions, differential pulse voltammograms (DPV) display a series of fairly regularly spaced, one electron-transfer peaks. The spacing ΔV is controlled by the capacitance per cluster C_{CLU} according to the simple relation $\Delta V = e/C_{\text{CLU}}$, where e is the electronic charge.

Quantized capacitance charging can also be observed for the arenethiolate-MPCs (PhC4SAu, PhC2SAu, and 4-CresolSAu) as demonstrated in Figure 1 (upper three panels). The resolution of the charging in the cyclic voltammograms shown is poor, but the differential pulse voltammetry (DPV) experiment clearly resolves multiple current peaks with magnitude well above background noise current levels. While some DPV peaks in Figure 1 may arise from extraneous faradaic background processes (such as that at +0.73 V for PhC4SAu), their overall number and regularity and the precedents of observations made on carefully fractionated samples^{10,15} make their interpretation as single electron quantized capacitance chargings rather obvious.

The arenethiolate-MPC results in Figure 1 further show that the quantized capacitance charging is not unique to MPCs protected by alkanethiolate dielectric shells^{10,15} and should be observable for additional kinds of protecting monolayers. The electrochemical quantized capacitance charging phenomenon can be anticipated to occur, in principle, for any nanoparticle of sufficiently small individual capacitance (i.e., small core size and surrounded by a medium of sufficiently small dielectric constant). It should be observable for clusters that are nominally not protected by monolayer shells (i.e., are "naked"), with the proviso that the approach of electrolyte ions (usually required in the medium in order to execute electrochemical experiments) to the nanoparticle surface not unduly increase its capacitance. An operational proviso is that the capacitance of the working electrode also be small, i.e., that the background currents be small.

Figure 2 lists the DPV peak positions²² derived from Figure 1. Figure 2 also gives MPC capacitances evaluated from the spacings ($\Delta V = e/C_{\text{CLU}}$) between peaks centered around the potential of zero charge of the clusters (ca.

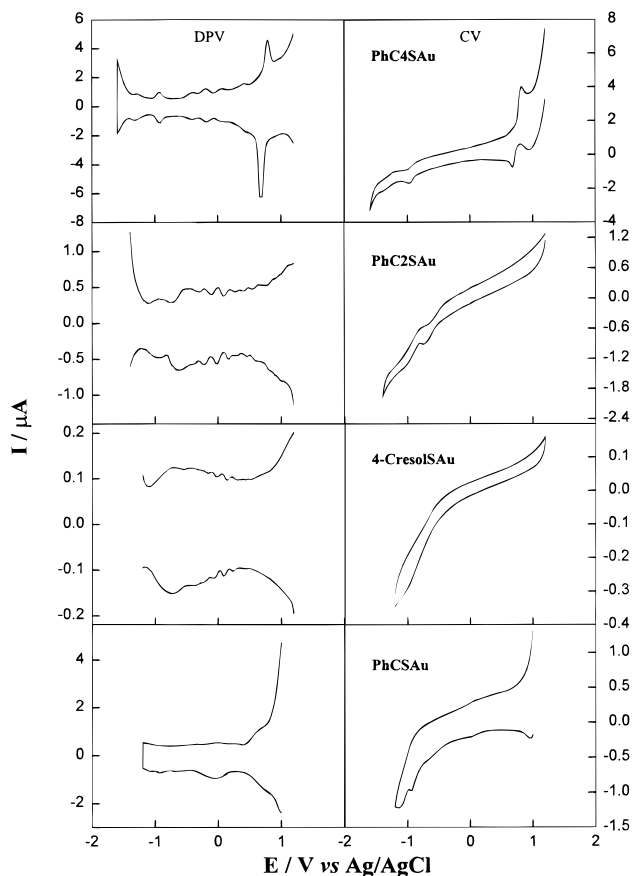


Figure 1. Differential pulse voltammograms (DPV, left-hand panels) and cyclic voltammograms (right-hand panels) of the indicated clusters in 0.05 M $\text{Hex}_4\text{NClO}_4$ in mixed solvent (2:1 v:v) toluene and acetonitrile. Concentrations (all in 3.0 mL solution): PhC4SAu, 20.8 mg; PhC2SAu, 7.9 mg; 4-CresolSAu, 6.8 mg; BenzylSAu, 10.5 mg. Pt disk electrode (0.063 cm^2) working electrode. DPV parameters: potential scan rate 10 mV/s; pulse amplitude 50 mV; pulse width 50 ms; pulse period 200 ms; sample width 17 ms. CV potential scan rate: 10 mV/s.

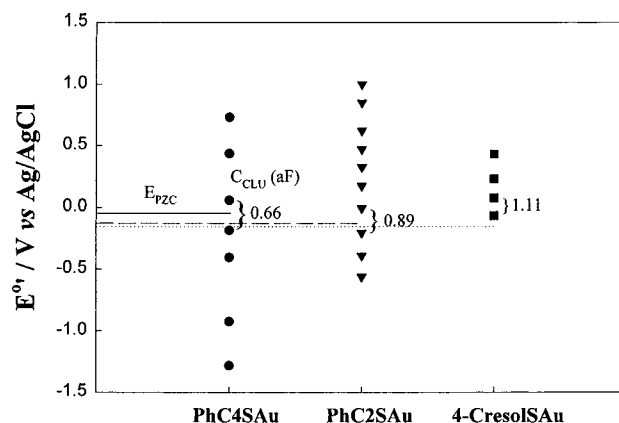


Figure 2. Peak potentials for the quantized capacitance charging features in the DPV curves of Figure 1. Numbers shown are the capacitances (aF/cluster) calculated from $C_{\text{CLU}} = e/\Delta V_C$ where ΔV_C is the peak spacing indicated (around the potential of zero charge of the MPCs, as established²³ by ac impedance of a monolayer of MPCs attached to an electrode; approximate E_{PZC} positions are indicated by dashed lines).

(20) Fan, F.-R. F.; Bard, A. J. *Science* **1997**, *277*, 1791.

(21) (a) Andres, R. P.; Bein, T.; Dorogi, M.; Feng, S.; Henderson, J. I.; Kubiak, C. P.; Mahoney, W.; Osifchin, R. G.; Reifenberger, R. *Science* **1996**, *272*, 1323. (b) Gerritsen, J. W.; Shafranuk, S. E.; Boon, E. J. G.; Schmid, G.; Vankempen, H. *Europhys. Lett.* **1996**, *33*, 279. (c) Hanna, A. E.; Tinkham, M. *Phys. Rev. B* **1991**, *44*, 5919. (d) Amman, M.; Wilkins, R.; Ben-Jacob, E.; Maer, P. D.; Jaklevic, R. C. *Phys. Rev. B* **1991**, *43*, 1146.

(22) The typical ΔE_{PEAK} separation between DPV peaks in forward and reverse potential scans (upper and lower curves in each panel) is less than 50 mV and likely represents effects of uncompensated solution resistance (iR_{UNC}) in the rather nonpolar solvent.

–0.2 V).²³ These peaks ostensibly correspond to changes in charge state of the clusters of $z = 0/+1$ and $0/-1$. The ΔV and C_{CLU} values for cluster capacitance are as follows: PhC4SAu MPC, $\Delta V = 0.24$ V, $C_{\text{CLU}} = 0.66$ aF/cluster; PhC2SAu MPC, $\Delta V = 0.18$ V, $C_{\text{CLU}} = 0.89$ aF/cluster; and

4-CresolSAu MPC, $\Delta V = 0.14$ V, $C_{\text{CLU}} = 1.11$ aF/cluster. These capacitances are somewhat larger than those (0.4–0.5 aF/cluster) of alkanethiolate Au MPCs prepared under similar conditions.¹⁰ The larger arenethiolate–MPC capacitances are consistent with their slightly larger core sizes and with the generally larger dielectric constants of aromatics relative to alkanes and may also reflect a greater intrusion of solvent and/or electrolyte ions (and hence a higher dielectric constant) into the monolayer.

The PhC4SAu MPC sample used for the DPV observations in Figure 1 had been fractionated by precipitation; DPV of this MPC in an unfractionated (as-prepared) state produced no obvious quantized charging pattern. Unfractionated PhCSAu preparations also gave featureless DPV results (exemplified by Figure 1, lowest panel). The PhC2SAu and 4-CresolSAu MPC samples were on the other hand, *unfractionated* materials, and their DPV results in Figure 1 are the first electrochemical quantized charging observations of as-prepared monolayer protected clusters. It was not evident in the previous experiments on alkanethiolate–MPCs^{10,15} that quantized charging results might be obtained without careful attention to obtaining core size monodispersity; this point was in fact stressed in our earlier work. The TEM images presented below make it clear that the PhC2SAu and 4-CresolSAu MPC samples are actually somewhat polydisperse. However, as discussed below, these materials contain a rather large proportion of small nanoparticles with a relatively narrow dispersity. The results in Figure 1 show that the proportion of MPCs of the smaller core size present in the mixture must be sufficiently large that their quantized charging events stand out despite the overall polydispersity of the sample. These are admittedly less well-defined samples, and quantized charging results on fractionated samples of the PhC2SAu and 4-CresolSAu MPCs would be valuable to obtain for comparison. Experiments to this end are in progress. However simulations of voltammetry of MPCs have shown^{10b} that quantized charging peaks should be observable even in polydisperse samples, near the potential of zero charge. At larger positive and negative potentials, the overlap of the different peaks due to different MPC capacitances blurs out the peaks. The Figure 1 DPV for PhC2SAu and 4-CresolSAu MPCs are just as the simulations anticipate; the most clearly evident peaks lie near the potential of zero charge (≈ -0.2 V).²³

Transmission Electron Microscopy (TEM). The metal core size, and dispersity thereof, of a MPC can readily be determined^{2,4} with TEM; illustrative results for various arenethiolate–MPCs are shown in Figure 3 and overall average results in Table 1. TEM images show⁵ that casting of dilute alkanethiolate–MPC solutions leads to semioordered islands and chains of clusters, with core–core spacings of uniformly about one alkanethiolate chainlength. Images of “naked” nanoparticles²⁴ of similar size have displayed a bilayer structure and unusual self-organization features of chains and rings where the top-layer nanoparticles rested in 2-fold saddle rather than 3-fold hollow sites, probably due to the balance between

local electrostatic repulsion and dispersion forces between neighboring particles. Arenethiolate–MPCs prepared under conditions of excess thiol occasionally show (Figure 3B–D) TEM images with chain/ring features, especially for arenethiols with the π -electron rich phenyl moiety close to the Au core (e.g., 4-CresolSAu, PhC2SAu, PhCSAu). Such self-organization is less evident in PhC4SAu MPC TEM images (Figure 3E), where individual nanoparticles are better-resolved, and for some reason the longer ligand promotes a decrease in interparticle interaction.¹⁸

Cast films of thiol-deficient preparations tend to contain a mixture of widely scattered MPCs and of clumps and patches of large (ca. 6 nm) MPCs (Figure 3A). Within the clumps, imaging is difficult. Such differences in morphology of the TEM samples probably reflects a complex amalgam of differing, polarity-based levels of adhesion of MPCs to one another and to the substrate surface during evaporation of the casting solvent and thus are tenuous to interpret in simple structural terms.

Measuring the core sizes of the arenethiolate–MPCs from the TEM images shows that they are relatively small nanoparticles (mean core sizes < 3 nm), and do not have a uniform core size. The Figure 3 insets show the core size distribution, and Table 1 gives results for the linear average of the population of nanoparticle diameters. Like alkanethiolate–MPCs,⁵ the average arenethiolate–MPC core diameters decrease strongly when prepared using reaction mixtures rich in thiol relative to gold. This dependency is qualitatively sensible, given that the eventual MPC core size is determined by the competing processes of core growth (following nucleation) and passivation against further growth by the encasing monolayer ligand shell. Larger excesses of thiol enhance the rate of passivation, yielding smaller nanoparticles.

The average arenethiolate–MPC core diameters depend on the specific arenethiol passivant, which is interesting in light of the relatively minor dependency of core size on alkane chainlength for alkanethiolate–MPCs^{5d} and are generally somewhat larger than alkylthiolate–MPCs (as shown by comparison to the C6SAu at the bottom of Table 1). Under identical reaction conditions, the MPC core size decreases with more methylene unit spacers between the aromatic moiety and the thiol reaction site (i.e., PhSAu $>$ PhCSAu \approx 4-CresolSAu $>$ PhC2SAu $>$ PhC4SAu $>$ C6Au), which may reflect a progression of capacities to passivate growth of the Au cores.

The distributions of arenethiolate–MPC core sizes (Figure 3) are also ligand-dependent, even under the same synthetic conditions (e.g., 0 °C, 3 \times). The distributions, or dispersities, of the 4-CresolSAu, PhC2SAu, and PhC4SAu MPCs core sizes are more narrow than those of alkanethiolate–MPCs,^{5d} and there are substantial populations of rather small clusters. The latter property stands out in their quantized charging (vide supra). The core size distributions can be *roughly* dissected into different populations. For example, for PhCSAu MPC, where the overall dispersity is substantial (Figure 3C inset), there appear to be six major populations centered at 1.2 (8%), 1.6 (21%), 2.5 (18%), 3 (15%), 3.7 (18%), and > 4.0 nm (20%). The distributions are narrower for the other three MPCs. PhC4SAu (Figure 3E inset) has populations (roughly) centered at 1.3 (19%), 1.8 (45%), 2.4 (16%), and > 3.0 nm (20%). Those for PhC2SAu (Figure 3D inset) are at 1.5 (24%) and 2.2 nm (76%), and those for 4-CresolAu (Figure 3B inset) lie at 1.5 (18%), 1.9 (19%), 2.6 (29%), 3.5 (14%), and > 4 nm (20%). For the latter three MPCs, the overall distributions can be also approximately modeled as a mixture of two populations, one having a smaller average core size and a narrow dispersity with the other

(23) The PZC of Au MPC was determined by ac impedance measurement of a monolayer of Au nanoclusters anchored on a Au electrode surface, by a local minimum of double-layer capacitance at ca. -0.2 V (vs Ag/AgCl), consistent with ref 10b, and by ac impedance measurements of self-assembled alkanethiolate monolayers on flat gold surfaces in the same organic medium by a shallow minimum in double-layer capacitance observed within the potential range of 0 to -0.4 V [Chen, S.; Murray, R. W., Unpublished results, 1997]. PZC for thiol monolayer-coated Au surfaces in a different medium (water) have been found^{12d} varying within a potential range as well ($+0.2$ to -0.4 V).

(24) Fink, J.; Kiely, C. J.; Bethell, D.; Schiffrin, D. J. *Chem. Mater.* **1998**, *10*, 922.

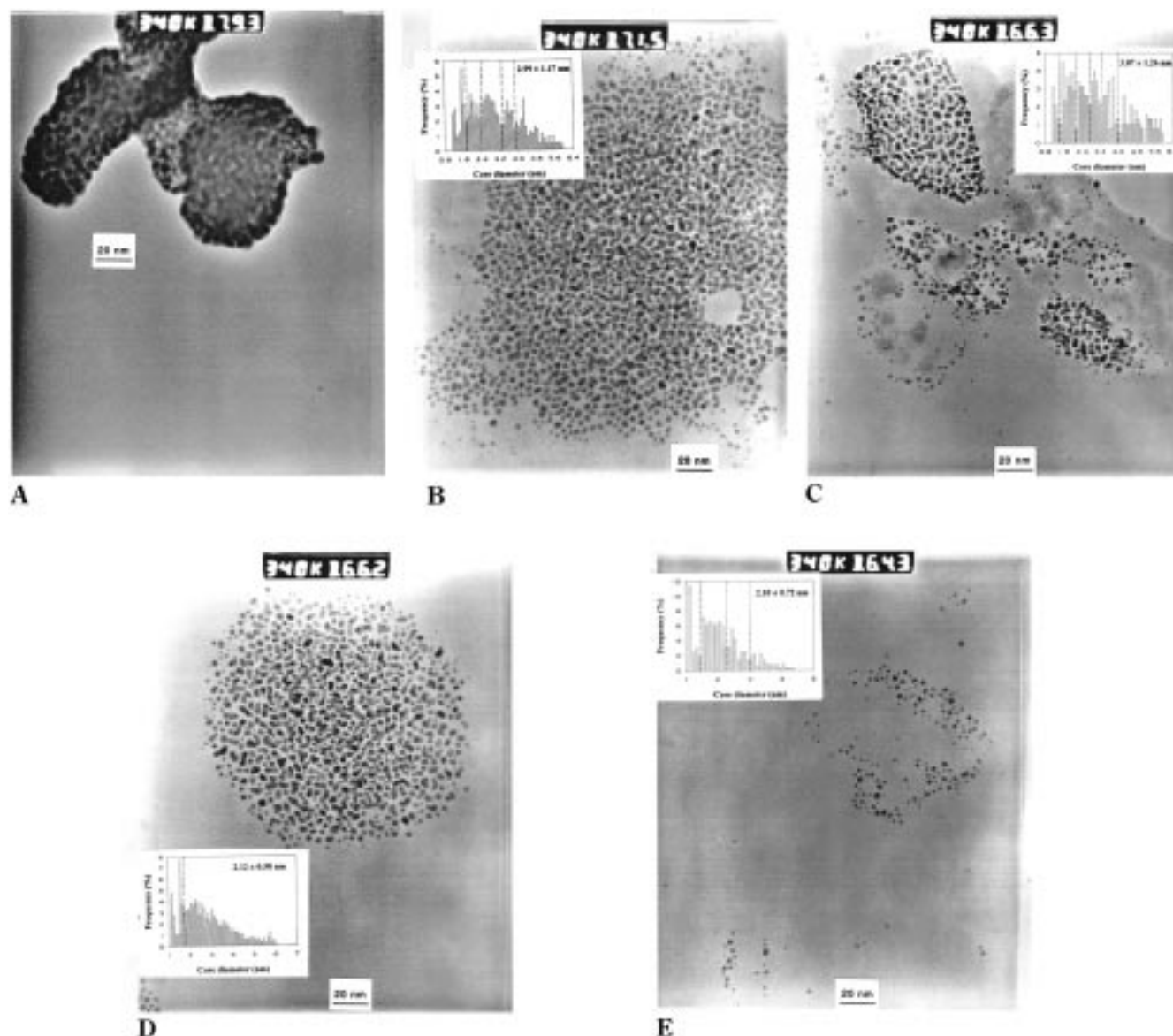


Figure 3. Transmission electron micrographs of cast films of various arenethiolate monolayer-protected Au clusters: (A) PhSAu (room temperature, $1/4\times$); (B) 4-CresolSAu (0 °C, $3\times$); (C) PhCSAu (0 °C, $3\times$); (D) PhC2SAu (0 °C, $3\times$); (E) PhC4SAu (0 °C, $3\times$). Insets show the corresponding distributions of core size with dashed lines indicating the separation of major populations.

Table 1. TGA and TEM Results for Arenethiolate Monolayer-Protected Clusters

Au MPCs	T_{DEC} (°C) ^a	TGA (% org.) ^b	S:Au ratio ^b	Avg. core dia. (nm) ^c	no. of Au (core shape) ^d [core surface area (nm ²)] ^d	no. of chains	no. of chains per unit surface area (nm ²)
PhSAu (room temperature, $1/4\times$)	238	8.8	0.17	6.5 ^e	9201 (TO)	1602	
PhSAu (room temperature, $1\times$)	232	8.3	0.16	6.5	9201(TO)	1494	
PhSAu (room temperature, $2\times$)	244	6.0	0.12				
PhSAu (0 °C, $3\times$)	226	12.6	0.26	(1.9) ^f	225 (TO ⁺) [15]	59	4.0
4-CresolSAu (0 °C, $3\times$)	226	16.7	0.32	3.0	976 (TO ⁻) [40]	316	7.9
2-NapSAu (0 °C, $3\times$)	269	22.8	0.37	2.1	309 (CO) [20]	113	5.8
PhCSAu (0 °C, $3\times$)	232	18.9	0.37	3.1	976 (TO) [40]	363	9.2
PhC2SAu (0 °C, $3\times$)	248	18.1	0.32	2.1	309 (CO) [20]	98	5.0
PhC4SAu (0 °C, $3\times$)	258	25.7	0.45	2.1	314 (TO ⁺) [19.5]	143	7.4
C6SAu (0 °C, $3\times$)	260	26.5	0.35	1.73	201 (TO) [15.2]	71	4.7

^a Temperature in TGA experiments corresponding to a 5% weight loss. ^b From percentage weight loss in TGA. ^c Determined by TEM. ^d Estimated as in ref 5d. CO = cuboctahedron shape; TO = ideal truncocuboctahedron (all sides equal); TO⁻ = truncocuboctahedron in which ($0 < n - m \leq 4$) where n is the number of atoms between (111) facets and m is the number of atoms between (111) and (100) facets; TO⁺ = truncocuboctahedron in which ($-4 \leq n - m < 0, m > 1$). ^e Average size of nanoparticles isolated from larger clumps is about 3.1 nm. ^f Estimated from about 30 isolated particles; most of the MPCs appeared to have decomposed and aggregated in the TEM micrographs.

with a larger average core size and a broad, overlapping dispersity. The latter characteristic is illustrated best by the PhC2SAu (Figure 3D inset) and PhC4SAu (Figure 3E

inset) MPCs and contributes to our ability to observe their electrochemical quantized charging behavior as discussed earlier. The above variations of core size dispersity must

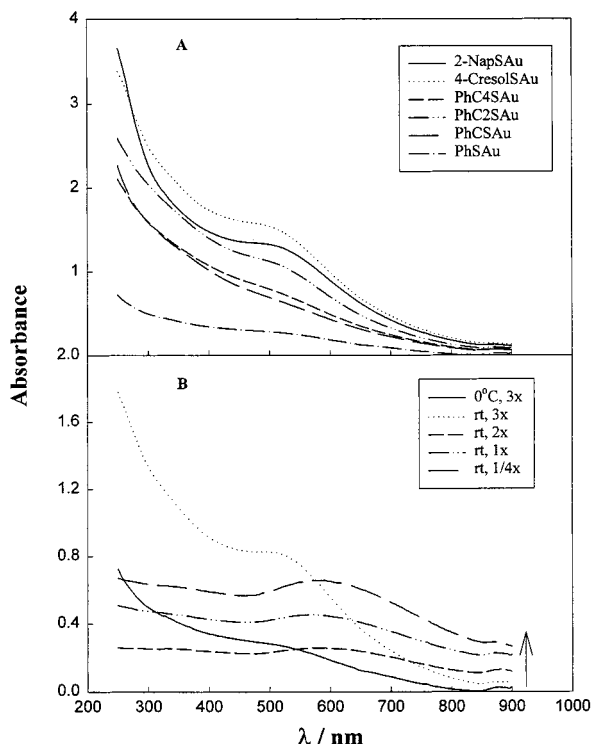


Figure 4. UV-Vis spectra of (A) arenethiolate-MPCs that had been prepared under the same conditions (0 °C, 3 \times) and of (B) PhSAu MPCs that had been prepared under different synthetic conditions. Solutions contain 1 mg MPC per 10 mL of CH₂Cl₂. Room temperature spectra were obtained.

reflect some differences in the as-yet poorly understood core nucleation/growth/passivation kinetics of these materials.

The resolution of the TEM images in Figure 3 (and of previous images of alkanethiolate-MPCs)^{5d} is insufficient to determine the core shape. Notwithstanding that the cluster-forming reaction potentially (owing to its intrinsically kinetically dominated character) leads to many MPCs with kinetically determined shapes, we have thus far relied on (and here continue to) calculations of energy-minimized core shapes,⁵ in which the likely equilibrium shape of alkanethiolate-MPC Au cores has been postulated to be a truncated octahedron (TO). We further assume that the core sizes are dominated by their tendency to form closed-shell structures (i.e., "magic numbers").⁵ On the basis of these two assumptions and the average TEM arenethiolate-MPC core sizes, and following a similar analysis^{5d} of alkanethiolate-MPC data, the most likely average number of Au atoms in the cores can be estimated. From

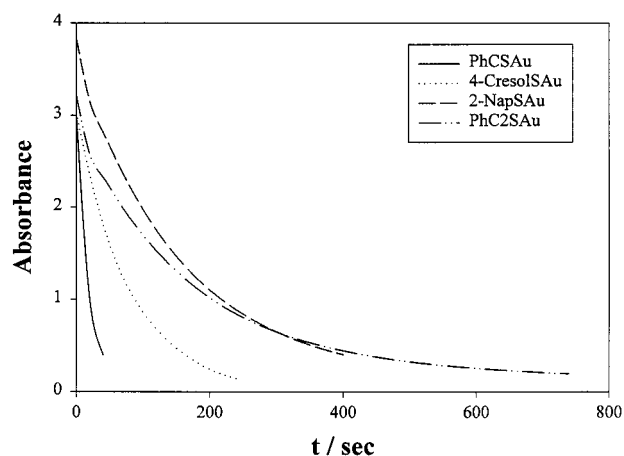


Figure 5. NaCN-induced decomposition of solutions of arenethiolate-MPCs, followed by absorbance measured at $\lambda = 520$ nm. [NaCN] = 8.70 mM; MPC concentration = ca. 7.1 mM.

the estimates given in Table 1, for instance, we see that the PhC4SH MPC, with the smallest average core size, is represented best by 314 Au atom truncated octahedral cores. Table 1 also gives the associated average core surface areas.

Thermogravimetric Analysis (TGA). Thermal decomposition of alkanethiolate-MPCs leads to volatilization of the organic fraction, as disulfides given thermal desorption mass spectrometry results,^{5d} leaving a residue of Au. The TGA results are consistent with elemental analysis.

TGA results for organic weight fractions of the arenethiolate-MPCs are given in Table 1. Taken with the average core size data, the TGA results yield the average number of arenethiolate ligands per MPC (no. of ligands) and the per unit core surface area. The ligand packing for alkanethiolate-MPCs is about 4.7 ligands/nm²; in comparison, the arenethiolates exhibit substantially higher packing densities. The 2-NapSH thiolate is a more bulky ligand than is the PhCS thiolate and thus reasonably exhibits a lower packing density. The higher arene-vs-alkanethiolate packing is at first glance surprising, but one must remember that the MPC surface is not flat but has a sharp curvature and a large proportion of edge and vertex sites.

Table 1 also lists the temperatures at which decomposition commences in the TGA experiment. Many of the arenethiolate-MPCs decompose at lower temperatures than those of *n*-alkanethiolate-MPCs, which are ca. 260 °C.^{5d} The 2-NapSAu and PhC4SAu MPCs are more thermally stable. The decomposition temperatures of

Table 2. Surface Plasmon Band Positions (λ_{MAX}) and the Aromatic IR Band Positions of Various Arenethiol-Stabilized Clusters (RSAu)

Au MPCs	UV-vis ^a surface plasmon λ_{MAX} (nm)	FTIR (cm ⁻¹)			
		(=C-H)	(C=C)		
PhSAu (room temperature, 1/4 \times)	575	3052	1573	1470	1435
PhSAu (room temperature, 1 \times)	575	3050	1573	1469	1435
PhSAu (room temperature, 2 \times)	579	3050	1573	1470	1436
PhSAu (room temperature, 3 \times)	525				
PhSAu (0 °C, 3 \times)	522	3051	1574	1469	1435
4-CresolSAu (0 °C, 3 \times)	518	3041	1593	1563	
2-NapSAu (0 °C, 3 \times)	520	3048	1619	1583	
PhCSAu (0 °C, 3 \times)	520	3058	1600	1493	1452
PhC2SAu (0 °C, 3 \times)	520	3059	1603	1495	1453
PhC4SAu (0 °C, 3 \times)	516	3060	1603	1496	1453
C6SAu (0 °C, 3 \times)	518				

^a From UV-vis spectra of ca. 1 mg MPC per 10 mL of CH₂Cl₂ solutions.

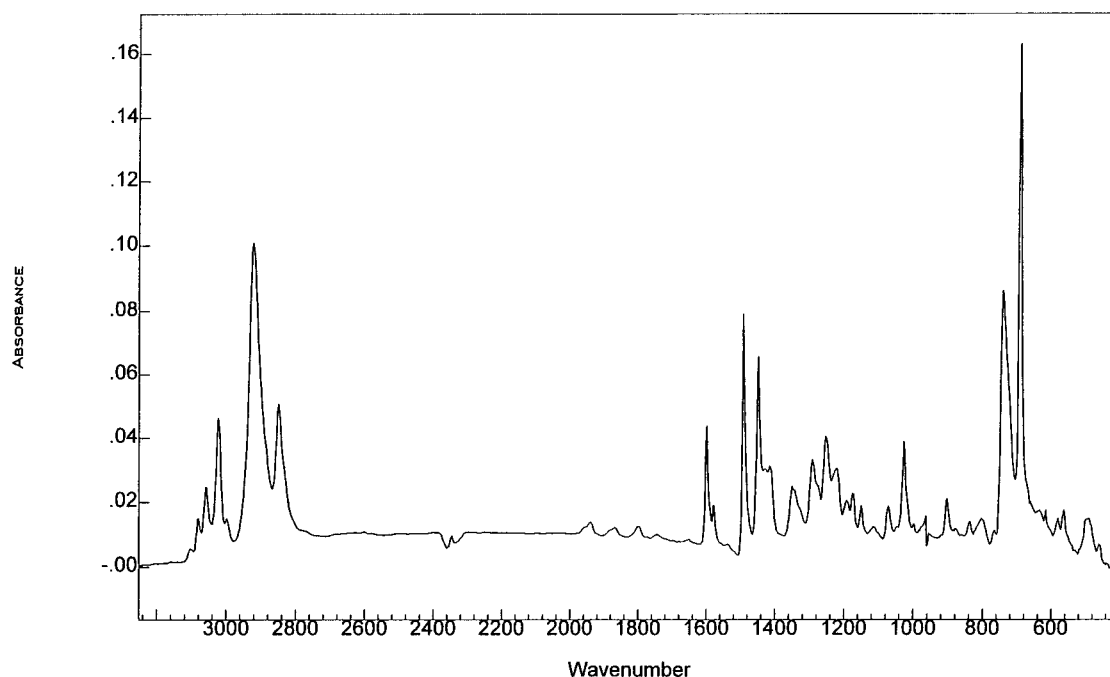


Figure 6. Transmission FTIR spectra of a film of PhC4SAu clusters dropcast onto a KBr plate.

clusters synthesized under similar conditions (0 °C, 3 \times) increase with methylene linker chain length (i.e., 4-CresolSAu \approx PhSAu < PhCSAu < PhC2SAu < PhC4SAu \approx C6SAu). There appears, however, to be no correlation between thermal stability and ligand packing density; i.e., high packing density does not confer thermal stability. There exists as yet no quantitative analysis of what determines thermal stability of thiolate-based Au clusters. Significant factors would be expected to include Au–thiolate bond energies, ligand–ligand packing energetics, the energetics of bond formation and volatilization of the disulfide products, and, possibly, the energetics of the ensuing nanoparticle aggregation.

UV–vis Spectroscopy. UV–vis absorption spectra (Figure 4A) of arenethiolate–MPCs display a smoothly increasing absorption at increasing energy (so-called Mie scattering), with a superimposed broad surface plasmon band between 500 and 600 nm. The plasmon band influences the visual colors of gold nanoparticles and arises^{25,26} from interband transitions between the highly polarizable Au 5d¹⁰ band and the unoccupied states of the conduction band. Table 2 lists the arenethiolate–MPC plasmon band positions. Clusters prepared under similar reaction conditions (0 °C, 3 \times , small cores) give plasmon bands at nearly invariant wavelengths (516–522 nm) that equal those reported for alkanethiolate–MPCs (518 nm).^{5d} It seems that, despite the quite substantial structural variations over these various stabilizing monolayers, the dielectric environment experienced by the gold core is little changed.

While the plasmon band energies in Figure 4A are independent of specific arenethiol ligands in preparations leading to relatively small core sizes (Table 2), their intensities at long wavelengths (Figure 4B, arrow) do vary systematically with the core sizes (Table 1), as has been before.^{5d,24} Additionally (Figure 4B and Table 2) show that PhSAu MPCs made under thiol-lean synthetic conditions (larger average core sizes result) exhibit plasmon bands

Table 3. Rate Constants of NaCN-Induced Decomposition of Arenethiolate–MPCs

Au MPC ^a	k_1 , s ⁻¹	k_2 , M ⁻¹ s ⁻¹
PhCSAu ^b	6×10^{-2}	10 ^c
4-CresolSAu	1.3×10^{-2}	1.5 ^c
PhC4SAu	6.6×10^{-3}	1.2 ^d
2-NapSAu	6.9×10^{-3}	0.80 ^c
PhC2SAu	3.5×10^{-3}	0.60 ^c
C6SAu	3.0×10^{-3}	0.52

^a All Au MPCs were synthesized at (0 °C, 3 \times). ^b Reaction was very fast; rate constants are estimates. ^c [NaCN] = 8.70 mM. ^d [NaCN] = 5.80 mM.

that are broader and lie at much lower energy (ca. 50 nm, or 0.21 eV). This could be partly accounted for by the formation of small aggregates of these MPCs as they demonstrated relatively poorer solubility. The electronic interaction between neighboring MPCs resulted in the observation of the collective band.²⁶

Kinetics of Cyanide-Induced Decomposition of Arenethiolate–MPCs. The chemical decomposition of Au MPCs allows another measure of the core-protecting capability of different ligands. We have established¹⁸ that cluster decomposition by cyanide in THF/water solutions gives predominantly disulfide products and (uncharacterized) colorless cyano–gold complexes. Our previous study¹⁸ of alkanethiolate–MPCs demonstrated that the reaction is first order in both MPC and cyanide. The experimental conditions are pseudo first order in MPC (a large excess of cyanide). The corresponding first-order relation (see Experimental Section) could be fit to the experimental absorbance–time results (Figure 5), provided a term for residual product absorbance (or scattering) of typically <0.3 was included. The nature of this residual absorbance is unknown, but it is a minor fraction of the experimental absorbances (Figure 5).

First- and second-order rate constant results are given in Table 3. The arenethiolate–MPC decomposition rate constants are overall larger than those of alkylthiolate–MPCs,¹⁸ and the decomposition rate constants seem correlated with ligand packing density; i.e., the higher the ligand packing density is, the faster the decomposition. This correlation is actually quite counterintuitive, which

(25) Alvarez, M. M.; Khoury, J. T.; Schaaff, T. G.; Shafigullin, M. N.; Vezmar, I.; Whetten, R. L. *J. Phys. Chem. B* **1997**, *101*, 3706.

(26) Bohren, C. F.; Huffman, D. R. *Absorption and Scattering of Light by Small Particles*; Wiley: New York, 1983.

might be due to the differential partition of CN^- into the monolayer shells as a result of the interaction between the phenyl moiety and the cyanide ion. The rate constants span a 20-fold range, with the least protection offered by the monolayer shell in PhCSAu MPCs and the most in PhC2SAu MPCs. For alkanethiolate-MPCs, values of k_2 decreased¹⁸ by 4-fold as the chain-length increased from C4 to C16, with that for the C6 alkanethiolate-MPC \approx the PhC2SAu MPC.

FTIR Spectra. An example of vibrational spectra of cast, solid-state films of arenethiolate-MPCs is given in Figure 6 for the PhC4SAu MPC (0 °C, 3 \times). The weak band at 3060 cm^{-1} is assigned to the aromatic =C-H stretch and those between 1400 and 1600 cm^{-1} to the ring C=C stretching bands. The data in Table 2 show that the aromatic =C-H stretching energy is higher when the aromatic ring is connected to a methylene linker as opposed to directly to the thiol site, but is otherwise relatively constant. The ring C=C stretching energies are quite variable for the three thioaromatic ligands (PhSAu, 4-CresolSAu, 2-NapSAu) and are relatively constant when the phenyl is bound through methylene linker chains of various lengths. There is no discernible effect of core size (in the PhSAu MPC series) on these vibration bands.

Summary

This study presents a new class of protecting monolayers for gold nanoparticles. Nanoclusters stabilized by arenethiol monolayers were synthesized by the Brust reaction⁴ and characterized by a variety of analytical techniques. Electrochemical quantized capacitance (Coulomb staircase) charging is observed using differential pulse voltammetry for three of the arenethiolate-MPCs. These features are observed in two cases even with crude,

unfractionated MPC samples, despite the polydispersity in core size established by TEM images. Cluster capacitances evaluated from the peak spacings between quantized charging peaks are somewhat greater than those of the alkylthiolate-MPCs. The Au core sizes of these MPCs were imaged by TEM and found to be slightly larger than those of *n*-alkanethiolate-MPCs that were synthesized under the same experimental conditions. The arenethiolate Au core sizes vary with the specific arenethiolate ligand, which is in contrast to *n*-alkylthiolate-MPCs where the core changes little with chainlength. Interesting self-organization features are observed in TEM images. TGA data show that the arenethiolate-MPCs are less thermally stable than their alkylthiolate counterparts; the thermal stability increases with longer methylene linkers. A counterintuitive trend is observed when decomposing clusters with cyanide; the reaction rate constants increase with ligand increasing packing density. UV-vis spectroscopic studies show that the surface plasma band position is virtually independent of the specific arenethiolate ligand while FTIR results revealed a spatial effect of the phenyl moiety on the intermolecular interaction between neighboring ligands in the protecting monolayers as well as that between the phenyl moiety and the Au core.

Acknowledgment. This research was supported in part by grants from the National Science Foundation and the Office of Naval Research. The authors thank Dr. J. DeSimone and Mr. S. M. Gross for providing access to the TGA instrument, and Drs. M. J. Hostetler and W. Ambrose (UNC Dental Research Center) for assistance in TEM measurements.

LA980817U